Out-of-equilibrium processes in suspensions of oppositely charged colloids: liquid-to-crystal nucleation and gel formation

Eduardo Sanz[1,2], **Chantal Valeriani**[1,2], **Teun Vissers**[1],
Andrea Fortini[1,5], **Mirjam E Leunissen**[1,6], **Alfons van Blaaderen**[1],
Daan Frenkel[3,4] **and Marjolein Dijkstra**[1]

[1] Soft Condensed Matter, Debye Institute for Nanomaterials Science, Utrecht University,
Princetonplein 5, 3584 CC Utrecht, The Netherlands
[2] SUPA, School of Physics, University of Edinburgh, JCMB King's Buildings, Mayfield Road,
Edinburgh EH9 3JZ, UK
[3] FOM Institute for Atomic and Molecular Physics, Kruislaan 407, 1098 SJ Amsterdam,
The Netherlands
[4] Department of Chemistry, University of Cambridge, Lensfield Road,
Cambridge CB2 1EW, UK

E-mail: esanz@ph.ed.ac.uk and M.Dijkstra1@uu.nl

Abstract

We study the kinetics of the liquid-to-crystal transformation and of gel formation in colloidal suspensions of oppositely charged particles. We analyse, by means of both computer simulations and experiments, the evolution of a fluid quenched to a state point of the phase diagram where the most stable state is either a homogeneous crystalline solid or a solid phase in contact with a dilute gas. On the one hand, at high temperatures and high packing fractions, close to a substitutionally-ordered/substitutionally-disordered solid-solid coexistence line, we find that the fluid-to-crystal pathway does not follow the minimum free energy route. On the other hand, a quench to a state point far from the substitutionally-ordered/ substitutionally-disordered crystal coexistence border is followed by a fluid-to-solid transition through the minimum free energy pathway. At low temperatures and packing fractions we observe that the system undergoes a gas–liquid spinodal decomposition that, at some point, stops, giving rise to a gel-like structure. Both our simulations and experiments suggest that increasing the interaction range favours crystallization over vitrification in gel-like structures.

(Some figures in this article are in colour only in the electronic version)

Colloidal suspensions are excellent model systems to study condensed matter physics. The reason is that colloids can be observed directly with current experimental techniques. In addition, colloids can form structures, such as colloidal crystals [1] or gels [2], that have potential applications, for instance, in photonics or in cosmetics. It is therefore essential to gain a better understanding in the physics governing the spontaneous transformation of a disordered fluid phase into a self-assembled colloidal structure. Here, we study how oppositely charged colloids assemble to form either crystals or gels. In particular, we are interested in the mechanism by which the fluid transforms into either phase. In our work, we make use of computer simulations to study the fluid-to-crystal transition, whereas

---

[5] Present address: Department of Physics, Yeshiva University, 500 West 185th Street, New York, NY 10033, USA.
[6] Present address: Center for Soft Matter Research, Physics Department, New York University, 4 Washington Place, New York, NY 10003, USA.

1

the gel formation has been studied both numerically and experimentally.

Quite recently, it has been demonstrated experimentally that a suspension of oppositely charged particles can transform into different crystal phases [1] and that the equilibrium phase diagram of a simple model potential for oppositely charged particles exhibits the same crystal structures found in experiments [3]. More recently, the gas–liquid coexistence line was calculated for the aforementioned model potential [4]. Taking advantage of the accurate knowledge of the equilibrium phase diagram we study the kinetics of both fluid–solid and fluid–gel transitions in oppositely charged colloidal suspensions.

The fluid-to-solid transition is an intriguing problem widely studied in colloid physics [5, 6]. The reason is that, by understanding the initial steps of crystal growth, one can aim to control the size and the structure of the crystallites eventually formed. The study of crystal nucleation in suspensions of hard colloidal particles has already received quite some attention both experimentally [6, 7] and in computer simulations [5, 8]. Other colloidal systems for which the liquid-to-solid transition mechanism has been studied are, for instance, equally charged particles [9, 10] or binary mixtures of hard spheres [11, 12]. Here, we present the case of oppositely charged particles. A special characteristic of the phase diagram of oppositely charged spheres is the coexistence between ordered and substitutionally disordered structures on a regular 3D lattice [3, 13]. This offers a good opportunity to study the role of an order–disorder phase transition in the liquid-to-solid nucleation pathway. We find that, in certain thermodynamic conditions, the formation of a disordered phase is kinetically favoured, whereas the nucleation of the ordered phase entails a lower free energy.

The formation of colloidal gels has also received a great deal of attention, not only because of the wide use of colloidal gels in cosmetics, drugs or food additives, but also because understanding gelation remains a fundamental challenge. The most popular system regarding colloidal gelation is that of colloid–polymer mixtures [14]. The presence of non-adsorbing polymers induces an effective attraction between the colloids, which is responsible for the gelation to happen [15, 16]. For the case of attractive particles, the mechanism by which a colloidal fluid transforms into a gel has been described as the arrest of a gas–liquid spinodal decomposition [2, 17, 18]. When a low density fluid separates into a very low density gas and a high density liquid by spinodal decomposition, a percolating pattern of dense liquid forms after the first steps of the spinodal phase separation. If the dynamics of the particles contained in the network-forming liquid is sufficiently slow, the pattern gets arrested, giving rise to a gel. Recently, it has been pointed out that mixtures of oppositely charged colloids can also form gels [19–21]. Hereby, we present experimental evidence confirming this statement. Moreover, we make use of computer simulations to gather evidence that the mechanism of gel formation for this system is an arrested spinodal decomposition, as is the case for purely attractive particles. Finally, we study, both numerically and experimentally, the role of the interaction range on the

interplay between vitrification and crystallization. Our results indicate that increasing the interaction range locally favours crystallization over vitrification.

1. Methods and technical details

1.1. Computer simulations

In the present work, we study a symmetric binary mixture of equally sized oppositely charged particles. The number of particles ranges from 686 (for the gel-formation simulations) to 8000 (for the Umbrella Sampling simulations). 1000 particles were used for the spontaneous nucleation and forward-flux-sampling (FFS) runs and for some of the gel-formation states.

In our computer simulations, the screened Coulomb interaction between two colloids of diameter σ and charge Ze is approximated by a Yukawa potential plus a repulsive core:

$$u(r)/k_{\mathrm{B}}T = \begin{cases} \infty & r < \sigma \\ \pm u^* \dfrac{\mathrm{e}^{-\kappa(r-\sigma)}}{r/\sigma} & \sigma \leqslant r < r_{\mathrm{c}} \\ 0 & r \geqslant r_{\mathrm{c}} \end{cases} \quad (1)$$

where r is the distance between the centre of mass of the colloids, u^* is the energy at contact in $k_{\mathrm{B}}T$ units and r_{c} is the cutoff radius (set at the distance where $u(r)/(u^* k_{\mathrm{B}}T) = 10^{-3}$). The energy in $k_{\mathrm{B}}T$ when $r = \sigma$, u^*, is equal to $Z^2 \lambda_{\mathrm{B}}/((1 + \frac{\kappa \sigma}{2})^2 \sigma)$, where $\lambda_{\mathrm{B}} = e^2/\epsilon_s k_{\mathrm{B}}T$ is the Bjerrum length (ϵ_s is the dielectric constant of the solvent) and $\kappa = \sqrt{8\pi \lambda_{\mathrm{B}} \rho_{\mathrm{salt}}}$ is the inverse Debye screening length for a 1:1 electrolyte (ρ_{salt} is the number density of added salt ions). To study the liquid-to-solid transition, we performed NPT Monte Carlo (MC) simulations using equation (1) as the Hamiltonian. In order to study the formation of gels, we performed Brownian dynamics (BD) simulations in the NVT ensemble, where we substituted the hard-core interaction of equation (1) by a steep u^*/r^{36} repulsion. Our units of energy and length are u^* and σ, respectively. Consequently, the time units are $t^* = \sigma^2/(D_0 u^*)$. The time step we used for the integration of the Langevin position equation [22] is $7 \times 10^{-6} t^*$.

Figure 1 shows a sketch of the equilibrium phase diagram for the model potential described by equation (1), in the u^*-colloidal-packing-fraction (ϕ) plane, calculated for $\kappa \sigma = 6$ [3, 4]. At low ϕ and u^*, the fluid is the most stable phase. At high ϕ, there exist several crystal structures. Two of them coexist with the fluid: a disordered face-centred-cubic solid (disordered fcc) at low u^* and a CsCl-like structure at high u^*. In the disordered-fcc solid, particles are arranged on an fcc lattice, but the sign of the charge each particle bears does not follow any order throughout the crystal. At high u^* the fluid–CsCl coexistence opens up and the solid coexists with a very low density fluid (gas). Buried underneath the gas–solid coexistence, there is a metastable gas–fluid coexistence line, which is denoted in the phase diagram by a dashed line. In our simulations, we quenched a stable fluid to the state points indicated by an asterisk and a letter in figure 1 and studied the structural evolution of the fluid in its way towards either a solid or a gel.

In order to observe a rare event such as crystal nucleation in a simulation of a modest number of particles it is necessary
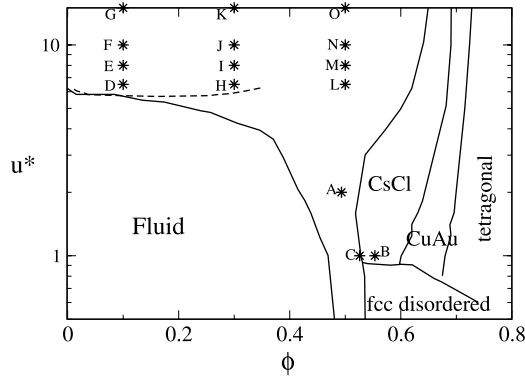
Figure 1. Phase diagram of equally sized oppositely charged particles (taken from [3] and [4]). The Hamiltonian is given by equation (1) ($\kappa\sigma = 6$). The solid lines indicate the coexistence lines, whereas the dashed line corresponds to the (metastable) gas–liquid binodal (solid–solid coexistence regions are too narrow to be visible on the scale of the figure). We have studied the structural evolution of a fluid when quenched to the state points indicated by an asterisk accompanied by a letter. The state points corresponding to each letter are the following: A: ($u^* = 2$, $\phi = 0.493$), B: ($u^* = 1$, $\phi = 0.553$), C: ($u^* = 1$, $\phi = 0.526$), D: ($u^* = 6.5$, $\phi = 0.1$), E: ($u^* = 8$, $\phi = 0.1$), F: ($u^* = 10$, $\phi = 0.1$), G: ($u^* = 15$, $\phi = 0.1$), H: ($u^* = 6.5$, $\phi = 0.3$), I: ($u^* = 8$, $\phi = 0.3$), J: ($u^* = 10$, $\phi = 0.3$), K: ($u^* = 15$, $\phi = 0.3$), L: ($u^* = 6.5$, $\phi = 0.5$), M: ($u^* = 8$, $\phi = 0.5$), N: ($u^* = 10$, $\phi = 0.5$), O: ($u^* = 15$, $\phi = 0.5$).

to use ad hoc simulation techniques. We have used two of them: umbrella sampling [23] and forward flux sampling [24]. The umbrella sampling method (US) involves biasing the sampling of an equilibrium MC simulation in order to explore high free energy configurations (containing large pre-critical clusters). We refer the reader to the review published in [10] for the method details. The forward-flux-sampling technique (FFS) uses an order parameter relevant for the transition to split the free energy landscape into regions divided by hyper-surfaces (or interfaces). In the FFS scheme, the calculation of the flux of formation of post-critical solid clusters in the liquid (number of post-critical clusters formed per unit of time and volume) is substituted by the flux of formation of small pre-critical solid clusters times the probability to form a post-critical cluster once one of these small pre-critical clusters has been formed. In contrast to the US method, FFS can also be used in strongly out-of-equilibrium situations, such as crystallization under shear [25]. FFS was applied for the first time to crystal nucleation to calculate the homogeneous crystallization rate in molten NaCl [26].

In order to study the liquid-to-solid transition path it is necessary to identify the particles belonging to a solid cluster. To do that, we use a local bond order parameter analysis [27]. In our study we compute the q_6 complex vector for each particle, which is a function of the relative orientation of a particle with respect to its neighbours (two particles are neighbours if they are closer than 1.33σ, the first $g(r)$ minimum). The component m of the vector associated with the ith particle is given by

$$q_{l,m}^i = \frac{1}{N_i} \frac{\sum_j^{N_i} Y_{l,m}(\mathbf{r}_{ij})}{(\mathbf{q}_l^i \mathbf{q}_l^{*i})^{1/2}}, \qquad m = [-6, 6] \qquad (2)$$

where, for our case, $l = 6$, N_i is the number of neighbours of particle i, and $Y_{l,m}(\mathbf{r}_{ij})$ is a spherical harmonic function whose form depends on l and m, and whose value depends on the relative orientation of particles i and j ($\mathbf{r}_{ij}$). In a perfect bcc or fcc crystal, all the particles have the same environment, and, therefore, the scalar product between the vectors of any pair of particles is 1. Two neighbouring particles are considered to be 'connected' if the scalar product of their normalized q_6 vectors exceeds a threshold of 0.7. If a particle has at least 9 connections it is labelled as 'solid'. Any two solid-like particles closer than 1.3σ belong to the same cluster. In this way we identify all solid clusters present in the metastable fluid phase (the size of the biggest one is the order parameter we have used to study crystal nucleation). It is important to note that our criterion to identify solid-like particles is blind to the type of solid lattice (bcc or fcc). This means that, by biasing the system to grow solid clusters with our solid criterion, we are not forcing the appearance of any particular solid structure.

To measure the degree of substitutional charge disorder within the growing solid clusters we use the following charge order parameter:

$$\xi = -\frac{1}{N} \sum_{i=1}^{N} \frac{1}{N_i} \sum_{j=1}^{N_i} \alpha_i \alpha_j \qquad (3)$$

where N is the number of particles in the solid cluster, N_i is the number of neighbours of particle i (for this purpose, a neighbour is any particle at a centre-of-mass distance closer than 1.12σ) and α is either $+1$ or -1, depending on whether the particle is positively or negatively charged. Thus, ξ is equal to 1 if all particles are surrounded by oppositely charged neighbours and -1 if all particles are surrounded by equally charged neighbours. Hence, for a perfectly ordered phase one should expect $\xi = 1$, whereas for a random phase ξ should be 0. Of course, when thermal fluctuations are present, ξ is lower than 1 even if the solid phase is ordered. However, on average, ξ will always be higher for a substitutionally ordered phase than for a disordered one. (Note that the threshold used to identify neighbouring particles here (1.12σ) is different from that used for the orientational order parameter described above (1.33σ). Both thresholds have been set to maximize the difference in order parameter value between either 'liquid' and 'solid' particles or substitutionally ordered and substitutionally disordered clusters.)

When studying crystallization at low and constant densities (NVT ensemble) we have used a looser criterion to detect solid-like particles. The reason is that in those conditions there are many particles at the interface between a dense phase and a gas phase. Obviously, an interface particle cannot have as many solid 'connections' as a bulk particle does. For us, a particle is solid-like if it is 'connected' to at least 50% of its neighbours. Two particles are 'connected' if the scalar product of their q_6 vectors is larger than 0.5. The neighbouring distances are defined in the same way as they were for the liquid-to-solid transition study at high densities (see above). We use the NVT ensemble for the study of the system's evolution at low densities because we are interested in the formation of gel-like structures. These structures

are formed in (gas–solid) coexistence regions of the phase diagram. Since in a *p*–*T* projection of the phase diagram there are not coexistence regions but coexistence lines, the *NPT* ensemble is not suitable if one desires to keep the system at coexistence.

1.2. Experiments

We used two different batches of polymethylmethacrylate (PMMA) particles, which were covalently labelled with the fluorescent dyes rhodamine isothiocyanate (RITC) and 7-nitrobenzo-2-oxa-1,3-diazol (NBD) and sterically stabilized with poly-12-hydroxystearic acid. We synthesized these particles by means of dispersion polymerization [28]. Both particle types were 2.5 μm in diameter, with a size polydispersity of 3%, as determined from static light scattering measurements.

We suspended the particles in a mixture of as-received cyclohexylbromide (CHB, Fluka) and 26.5% *cis*-decalin (Sigma-Aldrich) by weight. This mixture nearly matched the refractive index and density of the particles and had a dielectric constant of 5.6. We made suspensions with a 1:1 number ratio of the differently labelled particles at an overall volume fraction of $\phi \approx 0.10$, and either with (0.47 μM) or without the charge-determining tetrabutylammonium bromide salt (TBAB, Sigma-Aldrich) [1, 29]. In CHB, PMMA particles acquire a positive charge. When TBAB salt is added a fraction of the ions adsorbs onto the particle, with more of the small Br$^-$ ions adsorbing than of the large organic TBA$^+$ ions. The initial positive charge and the charge sign reversal point differ for each particle batch. We then made gradient samples by filling a glass capillary (Vitrocom) partially with the salt-free suspension and partially with the 0.47 μM TBAB suspension, and allowed it to form a macroscopic salt gradient over a couple of days' time. Suspending the particles in a salt gradient is a convenient way to quickly explore different experimental conditions. We studied these samples by means of confocal microscopy.

2. Results

2.1. Homogeneous crystal nucleation at high temperature and constant pressure

The most widespread view of crystal nucleation is that provided by classical nucleation theory (CNT) [30]. According to CNT, the formation of a crystal nucleus in a metastable liquid costs free energy due to the formation of an interfacial area A. On the other hand, the fact that the solid's (sol) chemical potential (μ) is lower than that of the metastable fluid (mf) is the driving force for crystal nucleation, and lowers the free energy of crystal formation. The balance between these two terms gives rise to a free energy barrier (ΔG):

$$\Delta G = A\gamma - n|\mu_{\text{sol}} - \mu_{mf}| \qquad (4)$$

where γ is the average liquid–solid surface free energy and n is the number of particles contained in the largest solid cluster. Because of the nucleation barrier, a (metastable) fluid can exist

at state points of the phase diagram where the solid has a lower chemical potential. Given that a metastable fluid is a quasi-equilibrium state, equilibrium thermodynamic statistics can be applied to study its properties. This allowed Duijneveldt and Frenkel to develop the US method to calculate nucleation free energy barriers [31]. The US method relies on the assumption that pre-critical clusters are in quasi-equilibrium with the surrounding liquid. Hence, it is possible to use any kind of MC sampling scheme to analyse the cluster's properties (structure, shape, critical cluster size, etc) via a US scheme. Here, we use two types of MC simulations to study the properties of the pre-critical clusters: (i) MC *NPT* simulations, in which volume moves and single-particle displacements are used to sample the configurational space and (ii) MC *NPT* simulations with charge swap moves, in which, besides the volume and particle moves, we occasionally try (20% of the times) to swap the positions of two oppositely charged particles. As mentioned before, as long as the quasi-equilibrium assumption holds, the properties of the clusters should not be affected by the way the system is sampled.

The US sampling scheme is tailored for conditions at which there is a high free energy barrier (a few tens of $k_\text{B}T$s) separating the metastable fluid and the solid. If the free energy barrier is not too high nor too small (otherwise there would not exist a metastable liquid) one can observe the liquid-to-solid transition without any biased simulation technique. This is precisely the case of state-point A, which is analysed in figure 2. Figure 2(a) shows the evolution of the internal energy per particle for two MC simulations (with and without charge swap moves) starting from a state-point-A metastable fluid configuration. After an initial stage in which the energy fluctuates around an average value (metastable liquid), the liquid transforms into a solid—as the energy drop proves. The solid formed in both cases (with and without charge swaps) corresponds to the stable phase at the state-point A: CsCl. Let us now analyse the nucleation pathway in more detail. In particular, we focus on the size and charge order of the largest cluster. Figure 2(b) shows the charge order parameter as a function of the size of the largest solid cluster along the transition path for both types of simulations. No significant difference is found between the two cases. Hence, the way the system is sampled does not affect the nucleation path in state A, confirming the hypothesis that clusters are at any time in quasi-equilibrium with the surrounding metastable liquid. Nothing unexpected has been observed for the study of state-point A.

Now we focus our attention on state-point B (also at a supersaturation high enough so as to allow nucleation to occur spontaneously in the course of a regular *NPT* simulation). In contrast to state-point A, there is competition between CsCl and disordered fcc because of the proximity of state B to the solid–solid coexistence line. Figure 3 shows a different scenario as compared to the case of state A. Depending on the MC simulation type, the metastable fluid ends up forming either an ordered-CsCl phase (with charge swap moves) or a disordered-fcc lattice (without charge swap moves). Note that the energy of the disordered-fcc solid (formed in the absence of swap moves) is higher than that of the liquid, indicating the entropic character of the phase transition. The number
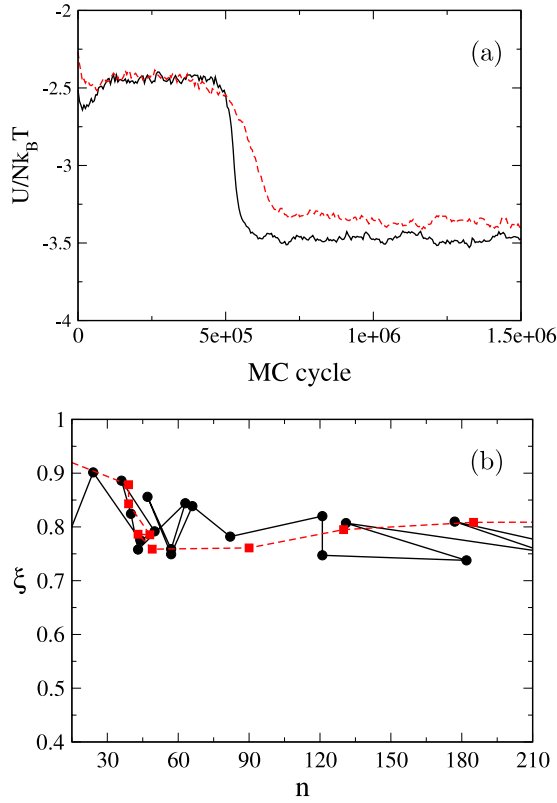
Figure 2. (a) Internal energy U versus the number of MC cycles and (b) charge order parameter ξ versus the number of particles in the largest solid cluster, n, for two liquid-to-solid trajectories, where the line connects two consecutive points along the trajectory. All results are obtained from two MC NPT simulations at state-point A. The solid lines (circles) correspond to the sampling without charge swaps and the dashed lines (squares) to the sampling with swaps.

of particles in the largest solid cluster, n, as a function of the number of MC cycles is shown in figure 3(b). We have analysed the solid clusters when n starts to grow continuously in size (indicated by an arrow in figure 3(b)). Figure 3(c), representing the charge order parameter as a function of the cluster size along the nucleation pathway, shows that not only is a different phase obtained by changing the sampling, but also that the nucleation path is different: if no charge swap moves are included in the MC simulations solid clusters have a noticeably lower charge order parameter. This is an indication that a kinetic effect is playing an important role in the crystallization path. If the transition path was solely determined by the underlying free energy landscape, pre-critical clusters would have had the same charge order parameter, regardless of the sampling scheme.

Some of the authors have recently reported a study of the liquid-to-solid transition at state-point C [32], which is in line with the observations described here for state B. Since the supersaturation at state-point C is lower than at B, a rare event simulation technique was required to observe the liquid-to-solid transition in computer simulations. Using the FFS technique we observed that the structure of the clusters along the transition path depends on the sampling scheme. If charge swap moves are included, the radial distribution function of the particles in the cluster reveals a CsCl-like structure, whereas
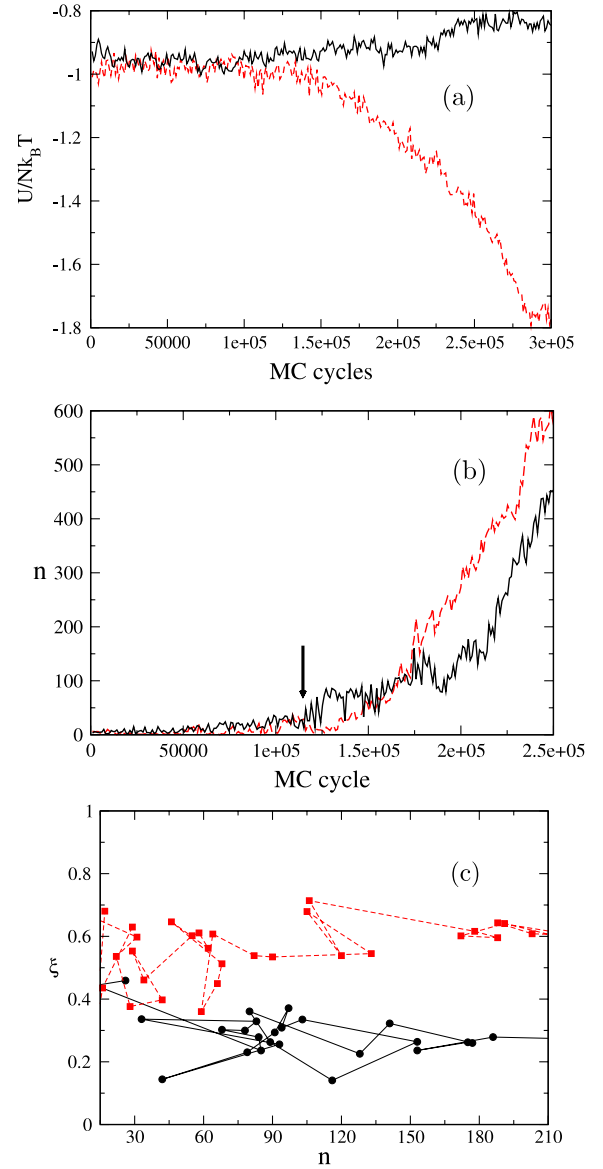

Figure 3. (a) Internal energy U versus number of MC cycles, (b) number of particles in the largest cluster, n, versus number of MC cycles, where the arrow indicates the point beyond which the liquid-to-solid trajectory has been analysed and (c) charge order parameter ξ versus number of particles in the largest solid cluster, n, for two liquid-to-solid trajectories, where the line connects consecutive points along the trajectory. All results are obtained from two simulations at state-point B. The solid lines (circles) correspond to the sampling without charge swaps and the dashed lines (squares) to the sampling with swaps.

an fcc lattice is observed otherwise [32]. Figure 4 shows the charge order parameter versus the number of particles in the largest solid cluster for two typical transition paths obtained in the FFS calculations. Confirming the study at state-point B, the path obtained with charge swap moves contains clusters with higher charge order. For small clusters the value of ξ is similar. Therefore, the difference between the two paths is not determined by the initial fluctuations towards the solid, but rather by the way particles are incorporated into the growing cluster. In order to grow an ordered cluster, particles have to be incorporated with a given charge sign at a given location at
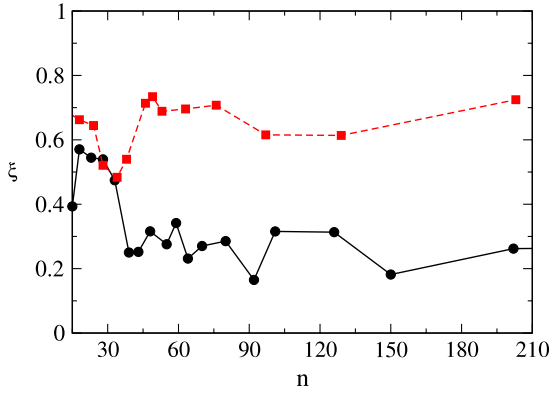
Figure 4. Charge order parameter ξ versus number of particles n in the largest solid cluster for two liquid-to-solid trajectories at state-point C (both calculated by means of the FFS method [24, 32]) with (squares) and without (circles) charge swap moves. The line connects consecutive points along the trajectory.

Figure 5. Gibbs free energy ΔG as a function of cluster size n for CsCl-ordered clusters (lower barrier) and for disordered-fcc clusters (higher barrier) [32]. A typical configuration of each type of cluster (disordered-fcc or ordered-CsCl) is shown in the figure. Green (light grey) and red (dark grey) particles are oppositely charged (colour online).

the cluster surface before the cluster itself re-dissolves. This condition is only fulfilled if swap moves are included.

In a recent paper, we have calculated the free energy barrier associated with each type of cluster (ordered-CsCl/disordered-fcc) via US simulations [32]. The barriers are shown in figure 5. We can grow either ordered or disordered clusters by respectively including or leaving out charge swap moves in the US MC simulation. This allows us to calculate the free energy associated with each path. As figure 5 shows, a path containing disordered-fcc clusters has a higher free energy. Since the US scheme is based on equilibrium simulations, the minimum free energy path should be eventually reached even if the system is inefficiently sampled (not including charge swapping). In fact, for a window centred around 30 particles (the size beyond which the free energy associated with each type of path diverges), around 3×10^5 MC cycles are required to complete a transition from disordered to ordered clusters. This 'time' is much larger than the time it takes for the clusters to grow and follow either type of path (see figures 3(b) and (c)). Therefore, without charge swap moves, the clusters keeps growing with charge disorder with no time to equilibrate to the lowest free energy path.

In summary, the simulations show that both for states B and C the transition path depends on the mobility of the particles. A possible interpretation is that, without the charge swap moves, the fluid is not ergodic on the timescale of cluster growth, not allowing for a minimization of the free energy of the path. The Stranski–Totomanow [33] conjecture, which states that the critical cluster structure is dictated by the lowest free energy barrier, is not compatible with our observations. For the system we present here, the mobility of the particles, and therefore the ability to equilibrate, not only determines which phase is eventually formed, but also the transition path.

Since the no-charge-swap sampling is obviously more realistic in terms of dynamics, we expect that, if an experiment were to be carried out under the same thermodynamics conditions, the system would follow the high free energy route of disordered-fcc clusters. We have confirmed by means of BD simulations—which provide a more realistic description of
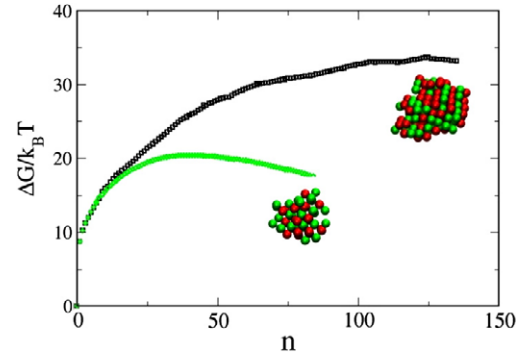
the dynamics than MC simulations—that a liquid quenched to state-point B transforms into a disordered-fcc solid.

2.2. Crystallization versus vitrification at low temperature and constant volume

So far we have presented results on the fluid-to-solid transition at high temperature and constant pressure. Let us now analyse how the fluid evolves when we quench the system to high u^* (low temperatures) at constant volume (state-points D–O). At the temperatures corresponding to state-points A–C the solid coexists with a high density fluid. By contrast, it coexists with a low density gas at the temperatures corresponding to states D–O. According to the equilibrium phase diagram, a BD NVT simulation starting from a homogeneous fluid quenched to states D–O should show how the system phase separates into a low density gas and a CsCl crystal. However, at the end of our simulations ($\sim 300t^*$) only state L became crystalline. In figure 6 the fraction of solid-like particles (see section 1 for the criterion to define a particle as 'solid-like') is plotted against time for the quenches at packing fraction 0.5 (states L–O). It is interesting to note that crystallization is only observed at state-point (L). This is somewhat counter-intuitive, since one expects faster crystallization for deeper quenches (higher thermodynamic driving force for crystallization). Hence, it must be the slowing down of the particles' dynamics that prevents the system from crystallizing at states M–O. We do not claim that crystallization will never take place at states M–O—it will eventually (as a diamond will eventually become graphite). We simply point out that the absence of crystallization within our simulation time for states M–O is not because of a high nucleation barrier, but because particles cannot move enough to rearrange into a crystalline lattice. Experiments [34], theory [16, 34, 35], and simulations [34–36] have confirmed the existence of an attractive glass for short-ranged attractive particles in a similar region of the phase diagram.

At lower packing fractions ($\phi = 0.1$ and 0.3, states D–K) there is no evidence of crystallization even after $\sim 1000t^*$.
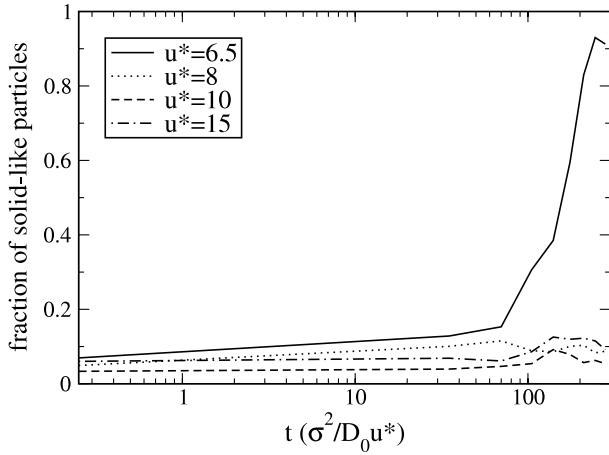
Figure 6. Fraction of solid-like particles as a function of time along the course of a BD NVT for states L–O (see figure 1). The starting configuration is a homogeneous fluid.
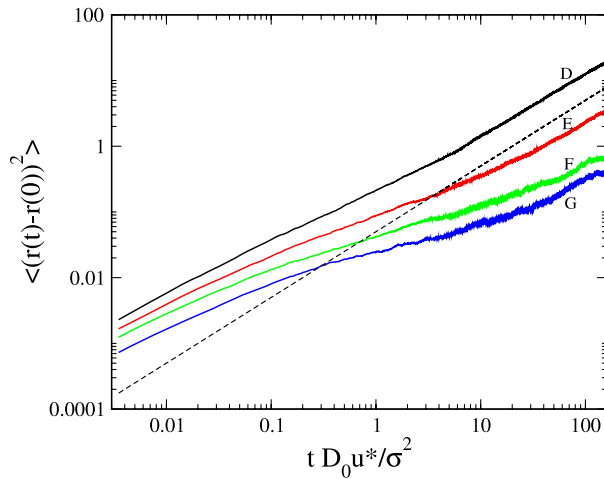

Figure 7. Mean square displacement $\langle (r(t) - r(0))^2 \rangle$ for the structures formed $950t^*$ after the quench to state-points D–G (see figure 1). The dashed line—just for visual reference—has slope 1.

Figure 7 shows that the mean square displacement calculated for the structures obtained $950t^*$ after the quench develops a clear inflection point on increasing u^*, which is a footprint of sub-diffusive dynamics. The referred slowing down of the particles' dynamics could be responsible for the absence of crystallization for quenches as deep as those to states G, K or O.

Figure 8 shows snapshots of the system at state-points G and K $500t^*$ after the quench. We remind the reader that the initial configuration of our simulations is a homogeneous fluid phase suddenly quenched to states G and K. Both configurations can be described as percolating networks of high density amorphous branches, which corresponds to the typical description of a gel. For a percolating network of dense amorphous branches to be a gel, it has to possess a non-zero yield stress. In a recent paper some of the authors have shown experimentally that oppositely charged colloids can indeed form gels [21]. In order to do so we imaged, by means of confocal microscopy, a colloidal network while
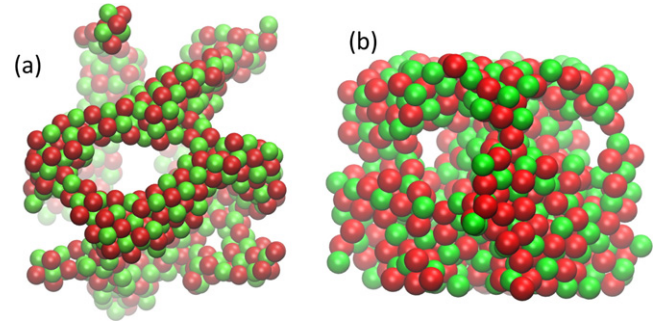

Figure 8. Snapshot of the structures obtained $500t^*$ after the quench to states G (a) and K (b). Green (light grey) and red (dark grey) particles are oppositely charged (colour online).

imposing a solvent flow through the sample. The network resisting the drag force exerted by the solvent demonstrates the ability of oppositely charged particles to form gels. In the same study, we demonstrated that the morphology of the gel-like configurations (figure 8) is due to an interruption of the metastable gas–liquid coexistence region [21]. In the equilibrium phase diagram, figure 1, there is a gas–liquid metastable coexistence buried underneath the gas–solid coexistence region. When a homogeneous fluid is quenched to states D–K a gas–liquid spinodal decomposition starts immediately. As soon as particles gather in high density regions, the spinodal coarsening process slows down because the local dynamics of the particles gets slow (due, in turn, to the high energy at contact and the short interaction range). The restricted mobility of the particles not only slows down the spinodal coarsening (giving rise to gel-like networks), but also prevents crystallization.

Finally, we analyse the influence of the range of the potential on the ability to crystallize. This information can be helpful for experimentalists, for making good colloidal crystals depends sensitively on numerous experimental variables [1, 37]. In order to assess the role of the interaction range on crystallization we have performed BD NVT simulations at the same packing fraction and u^* as states L–O but imposing a longer screening length ($\kappa\sigma = 2$ instead of 6). Starting from a homogeneous configuration we monitor the fraction of crystalline particles over time (see figure 9). Whereas for $\kappa\sigma = 6$ we only observed crystallization at $u^* = 6.5$ (figure 6), now the system readily becomes solid for $u^* = 6.5$, 8 and 10. Therefore, for the same contact energy, increasing the interaction range favours crystallization. This can be intuitively understood: particles in a dense amorphous phase need to rearrange in order to form crystalline domains; given that the attraction force is higher the shorter the interaction range (for a given u^*), rearrangements are easier for longer-ranged interactions. From an experimental point of view increasing the interaction range in a system of charged particles implies decreasing the amount of salt in the medium. Figure 9 also shows a manifestation of glassy particle dynamics (in the same way as figure 6 does for $\kappa\sigma = 6$). Again, on a thermodynamic basis, one would expect that increasing the contact energy favours the formation of the solid phase. In contrast, the system becomes glassy for high contact
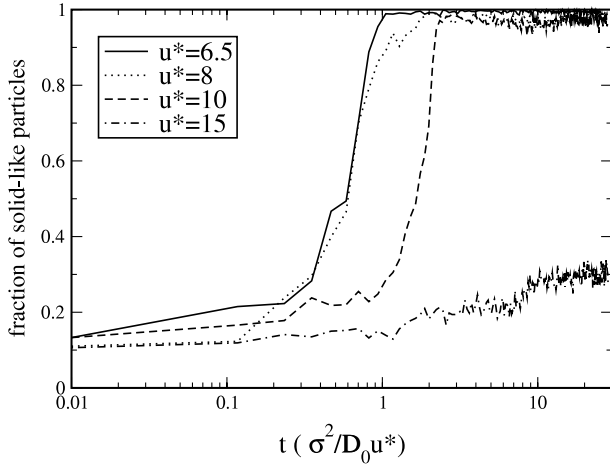
Figure 9. Same as figure 6 but with a longer interaction range: $\kappa\sigma = 2$ instead of 6.

Figure 10. A confocal microscopy image of a gel-like structure with amorphous branches readily formed after vigorously shaking the sample with a suspension of the two particle species. Green (light grey) and red (dark grey) particles are oppositely charged (colour online).

energies and crystallization gets hindered. For the quench at $u^* = 15$, a crystal cluster of ∼250 particles forms at the initial stage of the simulation. The fact that this crystalline domain cannot propagate throughout the simulation box is an indication that the system has fallen out of equilibrium.

As shown above, at low ϕ the system forms a percolating network of dense amorphous branches when quenched to a metastable gas–liquid coexistence point. In view of our observations for $\kappa\sigma = 2$ it is reasonable to expect crystallization within such amorphous branches at larger screening lengths. In that case, a percolating network of crystalline branches would result. Such a structure has already been observed for attractive particles [38–40]. Some of us have recently studied the case of $\kappa\sigma = 2$ at packing fraction 0.1 for contact energies ranging from $u^* = 12.5$ to 30 [21]. At $u^* = 20$ we found that about 15% of the system was crystalline; for the rest of the investigated states the system remained amorphous by the end of our simulations. Nevertheless, we show in our experiments (see section 1.2) that it is possible to obtain a percolating network of crystalline branches for oppositely charged particles (figure 11). In the experiments, we observed a percolating network of amorphous branches (figure 10) minutes after putting in contact both low- and high-salt concentration suspensions. These gels were observed in the high-salt-concentration half of the sample (particles are not oppositely charged in a free-of-salt environment [1]). Two days later, when the salt gradient had smoothened, we observed that the branches had coarsened and (partially) crystallized (figures 11(a) and (b)). Hence, the formation of percolating crystalline structures is due to local crystallization in the course of a metastable spinodal decomposition (by analogy with an amorphous branches' gel, whose formation can be described as vitrification in the course of a metastable spinodal decomposition). Further experimental work needs to be done to more accurately determine how far apart the timescales of gelation and crystallization actually were, as this was not investigated yet. In contrast to the experiments shown here, in a recent work, we did not observe crystallization in the branches of oppositely-charged-particles' gels [21]. An
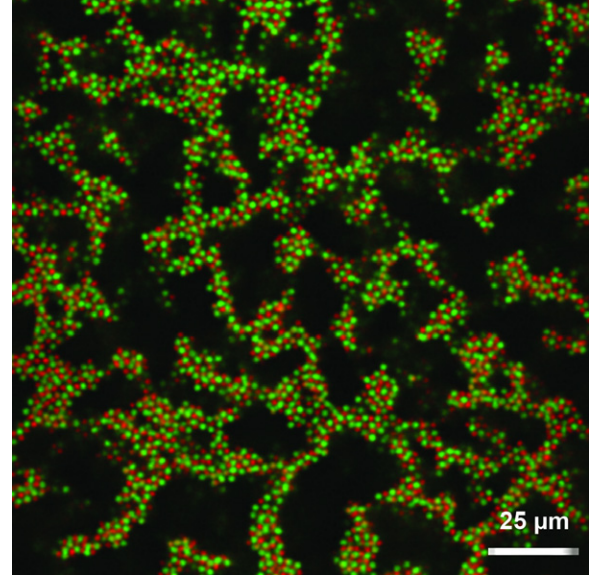
important difference between the two experimental systems was the amount of salt present in the medium. In the current experiments there is initially a salt gradient along the sample (0.47–0 μM). Hence, the average salt concentration was ∼0.23 μM, whereas it was 1 μM for the experiments reported in [21]. The particles' size was 2.5 μm for the present experiments (pr) and 2 μm for the former ones (for). Using the Derjaguin–Landau–Verwey–Overbeek (DLVO) [41, 42] approximation for κ ($\kappa = \sqrt{8\pi\lambda_B\rho_{salt}}$) we can estimate the ratio between both $\kappa\sigma$: $\kappa\sigma_{for}/\kappa\sigma_{pr} \approx 1.7$. Therefore, the interaction range was larger for the present experiments. This is in agreement with our simulations, where we observe that crystallization is easier for $\kappa\sigma = 2$ than for $\kappa\sigma = 6$. Summarizing, both simulations and experiments suggest that colloidal crystals form more readily for systems with long screening lengths. However, more careful experiments need to be carried out, since in our experimental system the charges of the colloidal particles are coupled to the concentration of salt in the medium.

3. Conclusions

We present a study of the evolution of a fluid of oppositely charged particles after being quenched to a state point of the equilibrium phase diagram where either a solid or a solid coexisting with a gas is the stable phase.

First of all, we have studied, by means of Monte Carlo simulations at constant temperature and pressure, crystal nucleation for quenches to state points where the solid is the most stable phase. Interestingly, the crystallization path taken by a metastable liquid close to an ordered-solid/disordered-solid coexistence line depends on the simulations' sampling scheme. If a 'fast' sampling scheme is used (including charge
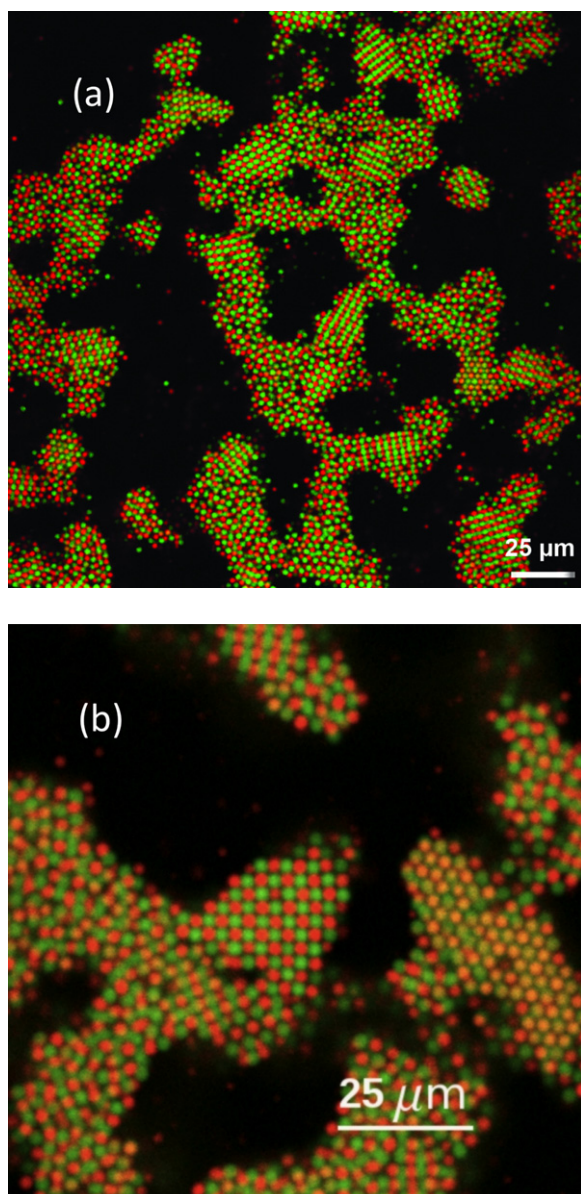
Figure 11. (a) A confocal microscopy image of a gel-like structure with crystalline branches observed two days after mixing. (b) A zoomed-in confocal image. Crystalline regions are observed in contact with amorphous ones.

swap moves), the nucleation path is a succession of ordered-solid clusters, while if a 'slow' sampling is performed (not including charge swap moves), the nucleation path contains disordered-solid clusters. By means of umbrella sampling calculations we have measured the free energy associated with each type of path: the free energy of the ordered-clusters path is lower than that of the disordered clusters. We interpret our results to indicate a lack of ergodicity of the slowly sampled fluid on the timescale of crystal growth. Our results contradict the Stranski–Totomanow conjecture, which states that the transition path is determined by the minimum free energy barrier for nucleation. For the case presented here, the mobility of the particles plays a major role in the selection of the nucleation path. We argue that, if an experiment were to be carried out under the same thermodynamic conditions, the system would follow the higher free energy route of disordered clusters. If the same study is repeated at a state point far away from the ordered-solid/disordered-solid coexistence line, the sampling scheme does not affect the transition path.

Secondly, we have studied the evolution of a fluid quenched to state points of the equilibrium phase diagram where a gas and a solid coexist. In order to do so, we have carried out Brownian dynamics simulations at constant volume and temperature. We observe clear signs of slow dynamics. For instance, the system does not crystallize faster for deeper quenches—which is what would be expected if crystallization is controlled by thermodynamics (nucleation free energy barrier). Moreover, the mean square displacement reveals sub-diffusive dynamics: a clear inflection point develops with the quench depth. The morphology of the system is very much influenced by the presence of a metastable gas–liquid spinodal: percolating networks of dense glassy branches (gels) are obtained as a consequence of the arrest of an ongoing spinodal decomposition. Finally, we have studied the influence of the interaction range on crystallization. Increasing the interaction range, while keeping the contact energy and the density constant, favours crystallization over vitrification. We believe this is the case because particles can rearrange more easily the longer the interaction range is. Nevertheless, the slow-dynamics footprint of crystallization being delayed by an increased quench depth is also present when the interaction range is increased. Crystallization in the experiments might be due, in agreement with our computer simulations, to an increase of screening length as the salt concentration decreases. However, this has to be further investigated, since the amount of charge on the particles is also correlated with the salt concentration in the system. Our work illustrates that either amorphous or crystalline-branched networks can be seen as an interrupted ongoing spinodal decomposition. In the former case, the interruption is due to vitrification, whereas in the latter it is due to crystallization.

Acknowledgments

References

[1] Leunissen M E, Christova C G, Hynninen A P, Royall C P, Campbell A I, Imhof A, Dijkstra M, van Roij R and van Blaaderen A 2005 *Nature* **437** 235
[2] Lu P J, Zaccarelli E, Ciulla F, Schofield A B, Sciortino F and Weitz D A 2008 *Nature* **453** 06931
[3] Hynninen A-P, Leunissen M E, van Blaaderen A and Dijkstra M 2006 *Phys. Rev. Lett.* **96** 018303

[4] Fortini A, Hynninen A and Dijkstra M 2006 *J. Chem. Phys.*
   125 094502
[5] Auer S and Frenkel D 2001 *Nature* **409** 1020
[6] Gasser U, Weeks E R, Schofield A, Pusey P N and
   Weitz D A 2001 *Science* **292** 258
[7] Harland J L and van Megen W 1997 *Phys. Rev.* E **55** 3054
[8] O'Malley B and Snook I 2003 *Phys. Rev. Lett.* **90** 085702
[9] Wette P, Schope H J and Palberg T 2005 *J. Chem. Phys.*
   123 174902
[10] Auer S and Frenkel D 2002 *J. Phys.: Condens. Matter* **14** 7667
[11] Henderson S I and van Megen W 1998 *Phys. Rev. Lett.* **80** 877
[12] Punnathanam S and Monson P A 2006 *J. Chem. Phys.*
   125 024508
[13] Bresme F, Vega C and Abascal J L F 2000 *Phys. Rev. Lett.*
   85 3217
[14] Asakura S and Oosawa F 1954 *J. Chem. Phys.* **22** 1255
[15] Poon W C K, Pirie A D and Pusey P N 1995 *Faraday Discuss.*
   101 65
[16] Bergenholtz J, Poon W C K and Fuchs M 2003 *Langmuir*
   19 4493
[17] Foffi G, Michele C D, Sciortino F and Tartaglia P 2005
   J. Chem. Phys. **122** 224903
[18] Buzzaccaro S, Rusconi R and Piazza R 2007 *Phys. Rev. Lett.*
   99 098301
[19] Romero-Cano M S, Caballero J B and Puertas A M 2006
   J. Phys. Chem. B **110** 13220
[20] Caballero J B and Puertas A M 2007 *Phys. Rev.* E **76** 011401
[21] Sanz E, Leunissen M E, Fortini A, van Blaaderen A and
   Dijkstra M 2008 *J. Phys. Chem.* B **112** 10861
[22] Allen M P and Tildesley D J 1987 *Computer Simulation of
   Liquids* (Oxford: Oxford University Press)
[23] van Duijneveldt J S and Frenkel D 1992 *J. Chem. Phys.*
   96 4655
[24] Allen R J, Warren P B and ten Wolde P R 2005 *Phys. Rev. Lett.*
   94 018104
[25] Allen R J, Valeriani C, Tanase-Nicola S, ten Wolde P R and
   Frenkel D 2008 *J. Chem. Phys.* **129** 134704
[26] Valeriani C, Sanz E and Frenkel D 2005 *J. Chem. Phys.*
   122 194501
[27] ten Wolde P R, Ruiz-Montero M J and Frenkel D 1996
   J. Chem. Phys. **104** 9932
[28] Bosma G, Pathmamanoharan C, de Hoog E, Kegel W,
   van Blaaderen A and Lekkerkerker H 2002 *J. Colloid
   Interface Sci.* **245** 292
[29] Royall C, Leunissen M and van Blaaderen A 2003 *J. Phys.:
   Condens. Matter* **15** S3581
[30] Kelton K F 1991 *Crystal Nucleation in Liquids and Glasses*
   (Boston, MA: Academic)
[31] van Duijneveld J S and Frenkel D 1992 *J. Chem. Phys.*
   96 4655
[32] Sanz E, Valeriani C, Frenkel D and Dijkstra M 2007 *Phys. Rev.
   Lett.* **99** 055501
[33] Stranski I N and Totomanow D 1933 *Z. Phys. Chem.* **163** 399
[34] Pham K N, Puertas A M, Bergenholtz J, Egelhaaf S U,
   Moussaid A, Pusey P N, Schofield A B, Cates M E,
   Fuchs M and Poon W C K 2002 *Science* **296** 104
[35] Puertas A M, Fuchs M and Cates M E 2002 *Phys. Rev. Lett.*
   88 098301
[36] Zaccarelli E, Sciortino F and Tartaglia P 2004 *J. Phys.:
   Condens. Matter* **2003** S4849
[37] Bartlett P and Campbell A I 2005 *Phys. Rev. Lett.* **95** 128302
[38] de Hoog E H A, Kegel W K, van Blaaderen A and
   Lekkerkerker H N W 2001 *Phys. Rev.* E **64** 021407
[39] Charbonneau P and Reichman D R 2007 *Phys. Rev.* E
   75 011507
[40] Smith P A, Petekidis G, Egelhaaf S U and Poon W C K 2007
   Phys. Rev. E **76** 041402
[41] Derjaguin B and Landau L 1941 *Acta Physicochim. URSS*
   14 633
[42] Verwey E J W and Overbeek J T G 1948 *Theory of the Stability
   of Lyotropic Colloids* (New York: Elsevier)